HHS Public Access

Author manuscript

Cell Rep. Author manuscript; available in PMC 2021 November 21.

Published in final edited form as:

Cell Rep. 2021 October 26; 37(4): 109897. doi:10.1016/j.celrep.2021.109897.

Adenosine deaminase 2 produced by infiltrative monocytes promotes liver fibrosis in nonalcoholic fatty liver disease

Shilpa Tiwari-Heckler[1,2], **Eric U. Yee**[3], **Yusuf Yalcin**[1], **Jiwoon Park**[4], **Duc-Huy T. Nguyen**[4], **Wenda Gao**[5], **Eva Csizmadia**[1], **Nezam Afdhal**[1], **Kenneth J. Mukamal**[6], **Simon C. Robson**[1,7], **Michelle Lai**[1], **Robert E. Schwartz**[4,*], **Z. Gordon Jiang**[1,8,*]

[1]Department of Gastroenterology, Hepatology and Nutrition, Beth Israel Deaconess Medical Center, Harvard Medical School, Boston, MA 02215, USA

[2]Department of Gastroenterology, University Hospital Heidelberg, Heidelberg, Germany

[3]Department of Pathology, University of Arkansas for Medical Sciences, Little Rock, AR 11794, USA

[4]Division of Gastroenterology and Hepatology, Weill Cornell Medical College, New York, NY, USA

[5]Antagen Institute for Biomedical Research, Boston, MA 02118, USA

[6]Division of General Medicine, Beth Israel Deaconess Medical Center, Harvard Medical School, Boston, MA 02215, USA

[7]Department of Anesthesia, Beth Israel Deaconess Medical Center, Harvard Medical School, Boston MA 02215, USA

[8]Lead contact

SUMMARY

Elevated circulating activity of adenosine deaminase 2 (ADA2) is associated with liver fibrosis in nonalcoholic fatty liver disease (NAFLD). In the liver of NAFLD patients, ADA2-positive portal macrophages are significantly associated with the degree of liver fibrosis. These liver

*Correspondence: res2025@med.cornell.edu (R.E.S.), zgjiang@bidmc.harvard.edu (Z.G.J.).

AUTHOR CONTRIBUTIONS

S.T.H., Z.G.J., and R.E.S. are responsible for the study concept, design, analysis, and interpretation of data; E.U.Y. and S.T.H. are main contributors the acquisition of data, while Y.Y., J.P., D.N., and E.C. provided supporting roles; W.G. and M.L. provided critical resources; Z.G.J. obtained main funding for the project, while R.E.S. and S.C.R. provided supporting role; S.T.H. and Z.G.J. wrote the first draft; E.U.Y., N.A., W.G., K.J.M., S.C.R., and R.E.S. provided critical revision.

SUPPLEMENTAL INFORMATION

Supplemental information can be found online at https://doi.org/10.1016/j.celrep.2021.109897.

DECLARATION OF INTERESTS

Z.G.J. is on the scientific advisory board of Olix Pharmaceuticals and receives grants from Pfizer and Gilead, Inc. R.E.S. is on the scientific advisory board of Miromatrix, Inc and is a consultant and speaker for Alnylam, Inc. However, the authors declare no conflicts of interest pertinent to this study.

INCLUSION AND DIVERSITY

We worked to ensure gender balance in the recruitment of human subjects, ethnic or other types of diversity in the recruitment of human subjects, and that the study questionnaires were prepared in an inclusive way. We worked to ensure sex balance in the selection of non-human subjects. One or more of the authors of this paper self-identifies as an underrepresented ethnic minority in science. The author list of this paper includes contributors from the location where the research was conducted who participated in the data collection, design, analysis, and/or interpretation of the work.

macrophages are CD14- and CD16-positive and co-express chemokine receptors CCR2, CCR5, and CXCR3, indicating infiltrative monocyte origin. Human circulatory monocytes release ADA2 upon macrophage differentiation *in vitro*. When stimulated by recombinant human ADA2 (rhADA2), human monocyte-derived macrophages demonstrate upregulation of pro-inflammatory and pro-fibrotic genes, including PDGF-B, a key pro-fibrotic cytokine. This PDGF-B upregulation is reproduced by inosine, the enzymatic product of ADA2, but not adenosine, and is abolished by E359N, a loss-of-function mutation in *ADA2*. Finally, rhADA2 also stimulates PDGF-B production from Kupffer cells in primary human liver spheroids. Together, these data suggest that infiltrative monocytes promote fibrogenesis in NAFLD via ADA2-mediated autocrine/paracrine signaling culminating in enhanced PDGF-B production.

Graphical Abstract

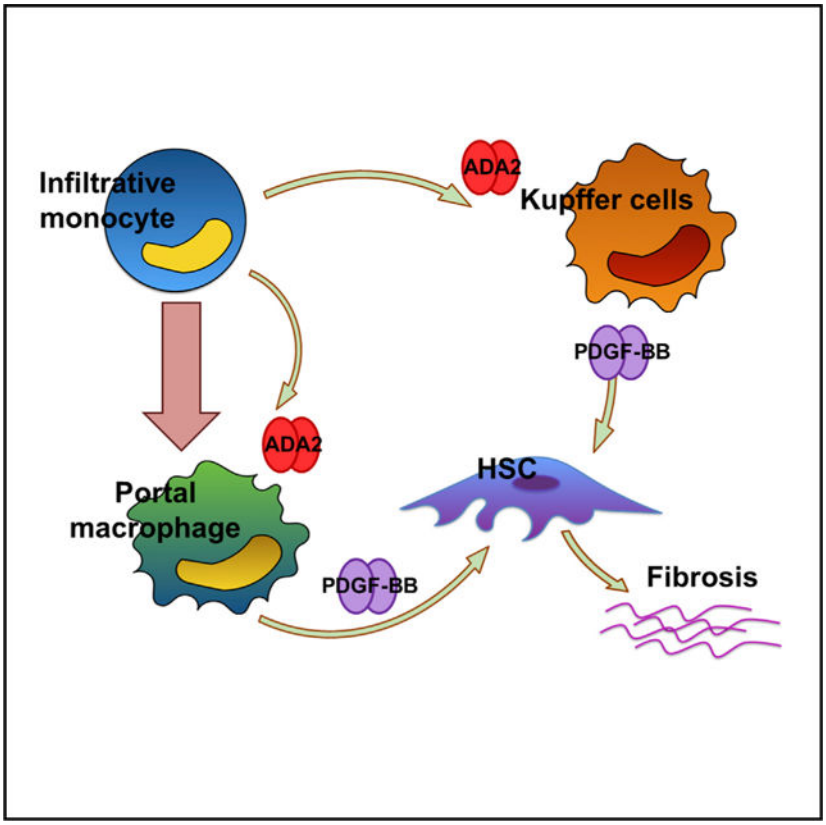

In brief

Tiwari-Heckler et al. find that infiltrative monocytes release ADA2 in NAFLD, which in turn promotes a pro-inflammatory and pro-fibrotic differentiation of monocyte-derived macrophages and Kupffer cells. This activity is at least in part dependent upon the deaminase activity of ADA2, inosine, the enzymatic product, and the production of PDGF-B.

INTRODUCTION

Nonalcoholic fatty liver disease (NAFLD) is the most common form of chronic liver disease and impacts up to one-third of adults in industrialized societies, such as the United States (Browning et al., 2004; Younossi et al., 2016). Despite its high prevalence, liver-related complications occur among selected patients who develop progressive liver fibrosis (Angulo et al., 2015). Fibrosis causes cirrhosis in approximately 5% of patients with NAFLD and represents the primary determinant of liver-related outcomes among NAFLD patients (Adams et al., 2005; Ekstedt et al., 2015). Hepatic steatosis causes metabolic injury to hepatocytes, which induces the production of extracellular mediators that activate myofibroblast precursor cells, and ultimately leads to liver fibrosis (Friedman, 2013). This process is amplified by various immune cells, among which infiltrative monocytes play a particularly important role (Tacke and Zimmermann, 2014). Intermediate $CD14^+/CD16^+$ monocytes are recruited to the liver during inflammation via CCL2, CCL5, and CXCL10 (Baeck et al., 2012; Miura et al., 2012; Zhang et al., 2014; Zimmermann et al., 2010). These infiltrative monocytes differentiate into macrophages and exhibit pro-inflammatory and pro-fibrotic dual properties, and induce the activation of hepatic stellate cells (Karlmark et al., 2009). This has led to the commercial development of drugs that inhibit monocyte chemotaxis for the treatment of fibrosis in NAFLD (Krenkel et al., 2018; Kruger et al., 2018). However, the molecular mechanism(s) that drives the pro-fibrogenic property of infiltrative monocyte-derived macrophages remains poorly understood.

Among the plexus of pathways that impact liver fibrosis, adenosine has long been recognized as a potent fibrosis mediator (Fausther, 2018). This concept is supported by the ample epidemiological observations that coffee consumption is associated with a lower risk of liver fibrosis (Saab et al., 2014). Caffeine, a nonspecific adenosine receptor antagonist, protects against liver fibrosis formation in animal models and is associated with protective effects in some human studies (Dranoff et al., 2014). Extracellular adenosine is derived from ATP, a potent pro-inflammatory signaling molecule that acts through P2X and P2Y receptors (Eltzschig et al., 2012). Extracellular ATP is converted to adenosine by ectonucleoside triphosphate diphosphohydrolase (ENTPD, CD39) and in tandem with 5′-nucleotidase (ecto-5′-NT, also known as CD73) (Antonioli et al., 2013; Deaglio and Robson, 2011). Adenosine is subsequently converted to inosine by adenosine deaminase (ADA). In the human liver, CD39 (ENTPD1) was found in endothelial and immune cells, ENTPD8 in hepatocytes, and CD73 in hepatocytes and endothelial cells (MacParland et al., 2018). Among the three enzymatic steps that convert ATP to inosine, the activity of the last deaminase step in the serum is robustly associated with liver fibrosis in NAFLD patients (Jiang et al., 2018). Humans have two isoforms of ADA: ADA1 and ADA2. It is the serum activity of the latter that drives the association with fibrosis. ADA2, also known as cat-eye syndrome chromosome region protein 1 (CECR1), is a secreted protein produced by activated monocytes and dendritic cells (Zavialov and Engström, 2005). Congenital mutations in ADA2 manifest clinically in various ways, from anemia to vasculitis and intracranial hemorrhage (Navon Elkan et al., 2014; Zhou et al., 2014). It has been shown that defects in ADA2 promote a pro-inflammatory macrophage differentiation *in vitro* (Zhou et al., 2014).

In this study, we aim to study the mechanism that underscores the association between ADA2 activity and liver fibrosis in NAFLD.

RESULTS

ADA2 is highly expressed by portal mononuclear cells in NAFLD

We first examined the expression of ADA2 in the liver. A total of 91 patients were identified from a cohort from which we originally identified the association between serum activity of ADA2 and liver fibrosis. These patients were selected for even distribution of the stage of liver fibrosis (Table 1). Immunohistochemistry staining of ADA2 on liver biopsy demonstrated three patterns of ADA2-positive ($ADA2^{pos}$) cells: mononuclear cells in the portal area, lobular inflammatory foci, and sinusoids (Figures 1A and S1). The $ADA2^{pos}$ cells in the portal area were typically large with the most intense ADA2 staining in the cytoplasm (Figure 1A, arrows). $ADA2^{pos}$ cells in the sinusoid were spindle-shaped, in keeping with the typical morphology of Kupffer cells (Figure 1A, arrowheads). $ADA2^{pos}$ cells in inflammatory foci appeared similar to those in the portal area. Histological scores were developed to rank the number of $ADA2^{pos}$ cells in these three distributions and study the relationship between ADA2 expression and NAFLD disease severity. We found that among the three distributions of $ADA2^{pos}$ cells, $ADA2^{pos}$ cells in the portal area correlated with the stage of liver fibrosis and histological scores of ballooning degeneration (Figures 1B and 1D). In the presence of bridging septal fibrosis, the scoring of $ADA2^{pos}$ cells in the portal area was more difficult, as the portal tract was harder to define. In comparison, the extent of $ADA2^{pos}$ Kupffer cells or cells in the lobular inflammatory foci, demonstrated a correlation with the histologic score of lobular inflammation, but not with the stage of liver fibrosis or ballooning degeneration (Figures 1B–1D). The extent of $ADA2^{pos}$ cells on the liver biopsy did not correlate with hepatic steatosis (data not shown). None of the three $ADA2^{pos}$-cell scores on the liver biopsy correlated with serum ADA2 activity. Instead, we found that serum ADA2 and the score of $ADA2^{pos}$ portal macrophages were independently associated with the stage of liver fibrosis (Table S1).

Infiltrative monocytes express and secrete ADA2 upon differentiation into macrophages

To determine the origin of $ADA2^{pos}$ cells in the liver, we performed immunofluorescent costaining of ADA2 and markers of macrophages and monocytes. $ADA2^{pos}$ cells in the portal area exhibited different markers compared to cells in the hepatic lobule. Portal $ADA2^{pos}$ cells demonstrated intense ADA2 immunofluorescent staining along with CD68, a macrophage marker (Figure 2A). $ADA2^{pos}$ portal macrophages were also double-positive for CD14, CD16, an immunophenotype of intermediate monocytes, and CCR2, CCR5, CXCR3, markers of infiltrative monocytes (Figure 2A). In contrast, the ADA2 staining on Kupffer cells in the hepatic lobule was weaker. These cells costained with CD16, but not CD14 or CD68 (Figure S2). These cells also co-expressed MARCO, a human Kupffer cell marker, and to a lesser extent, CCR5, but not CCR2 or CXCR3 (Figure S2). To further validate the origin of $ADA2^{pos}$ portal macrophages as intermediate ($CD14^{+}$/$CD16^{+}$) circulating monocytes, we examined ADA2 expression in circulating monocytes from human volunteers (Figure 2B). Most classical ($CD14^{+}$/$CD16^{-}$), intermediate ($CD14^{+}$/$CD16^{+}$), and non-classical ($CD14^{dim}$/$CD16^{+}$) monocytes expressed ADA2, yet intermediate

monocytes had the highest proportion of ADA2-positive cells and highest mean ADA2 expression level measured by fluorescent staining (Figure 2B).

We then performed *in situ* hybridization (ISH) for ADA2 using RNAScope to examine ADA2 transcription. In comparison to the immunohistochemistry of ADA2, mRNA transcripts of ADA2 were concentrated in cells in the inflammatory foci and portal tracts (Figure 2C). This raised the possibility that the production of ADA2 differs between infiltrative monocytes and Kupffer cells. To test whether the differentiation of monocytes into macrophages changed ADA2 production, we induced the differentiation of U937 monocytes to macrophages *in vitro* with phorbol myristate acetate (PMA). Upon differentiation, the intracellular ADA2 mRNA increased, but its protein level decreased in U937 cells. In the meantime, the activity of ADA2 in the media increased over time within 6 h, indicating the secretion of ADA2 upon differentiation (Figure 2D). The differentiation of human monocyte-derived macrophages (MoMF) induced by M-CSF *in vitro* was much slower. A similar decrease in intracellular ADA2 concentration was noted within 24 h, but this recovered to some extent over time (Figure 2E). The ADA2 activity was detected in the media throughout differentiation (Figure 2F). This would have led to a significant accumulation of ADA2 in the media (dashed line) if the media were not replaced every 2–3 days. Together, these observations indicated that macrophages differentiated from infiltrative monocytes actively secreted ADA2 and raised the possibility of an ADA2-mediated paracrine pathway.

Extracellular ADA2 induces pro-inflammatory and pro-fibrotic changes in macrophages

To understand the impact of ADA2 on macrophages, we cloned recombinant human ADA2 (rhADA2) with a six-histidine tag at the C terminus and expressed the protein in CHO cells. The protein was purified using nickel affinity chromatography from the culture media and confirmed by western blot (Figure S3). The purified rhADA2 was added to MoMF at 100 nM concentration (84 U/L) for 48 h (Figure 3A). RNA-seq of the cells demonstrated profound changes in transcriptomes induced by rhADA2. Among the 15,470 genes, a total of 1,836 were upregulated at least two-fold, and 1,099 downregulated at least two-fold with adjusted p values less than 0.001 (Figure 3B; Data S1 and S2).
We compared the transcriptional signature of rhADA2-treated and control macrophages with gene set enrichment analysis and found a significant enrichment of genes in the inflammatory response set with false discovery rate (FDR) *q*-values at 0.12 (FDR q values < 0.25 are considered significant) (Subramanian et al., 2005) (Figure S4A). Among these changes, ADA2 induced upregulation of pro-inflammatory cytokines: TNFα, IL1, IL10, IL6, chemokine profiles characterized by CCL1, 4, 5, surface markers CD80 and CD86, but downregulation of CD163, a pattern in keeping with an M2b differentiation (Figure 3C). This pattern was further validated in rhADA2 treated MoMF isolated from six independent volunteers (Figure 3D).

We then examined whether ADA2 impacts the release of pro-fibrotic cytokines by macrophages. RNA-seq analysis showed an increase in both TGFβ and platelet-derived growth factor B (PDGF-B). Among the two key pro-fibrotic cytokines, ADA2 significantly upregulated PDGF-B expression, but only a trend in the upregulation TGFβ mRNA was

noted ($p = 0.06$) in additional validation using MoMF from six individuals (Figure 3E). Similar ADA2-induced PDGF-B upregulation was seen in U937 differentiated macrophages. In the cell culture media, we observed an increase in the production of PDGF-BB dimer at 48 h by MoMF after ADA2 stimulation (Figure 3F). An ADA2 dose-dependent increase in PDGF-BB production was noted in U937 cells. This ADA2-induced PDGF-BB secretion was reproduced among MoMF. In comparison, we did not detect TGFβ in the media of U937 cells with or without ADA2 stimulation. In the human liver with NAFLD, the expression of PDGF-B was noted in portal macrophages ($CCR2^{+}/MARCO^{+}$), as well as Kupffer cells in the lobule ($CCR2^{-}/MARCO^{+}$) (Figure 3G).

Deaminase activity contributes to the impact of ADA2

To further understand the mechanism underlying the impact of rhADA2 on macrophage differentiation, we generated a rhADA2 mutant with no deaminase activity (Figure 4A). The active site of ADA2 is composed of charged residues E359, H112, H114, D115, H356, H382, and D477, supported by hydrophobic residues W204, F207, and F211, among which E359 is the proposed proton donor (Zavialov et al., 2010). Based on the structure, we mutated glutamate 359 to asparagine, a change that would inhibit proton transfer and abolish the deaminase activity but was unlikely to cause protein misfolding. As expected, CHO cells expressed and secreted E359N at similar levels as wild-type ADA2, indicating good protein folding. Purified E359N exhibited nearly no deaminase activity (Figure 4B). When rhADA2 E359N was added to the culture media of MoMF from healthy volunteers, E359N was not able to upregulate the transcription of TNFα, IL6, IL10, and PDGF-B transcripts as wild-type ADA2 could (Figure 4C). Similarly, we observed no accumulation of PDGF-BB in the culture media after 48 h (Figure 4D) in the presence of E359N mutants. MoMF stimulated by wild-type ADA2 resulted in upregulation of G-protein coupled receptor related genes and activation of AKT-PI3K-mTOR pathways as shown by gene enrichment analysis (Figures S4B–4D). This finding raised the possibility that ADA2 impacts adenosine/inosine mediated signaling.

To further test the role of deaminase activity, we compared the impact on macrophage phenotype of adenosine and inosine, the substrate and product of ADA2, respectively (Figure 4E). The RPMI media contained adenosine, and its concentration decreased after the culture of macrophages for 48 h. The supplementation of ADA2 did not change the adenosine concentration and significantly increased the concentration of inosine in the harvested media (Figure 4F). These concentrations likely reflect an equilibrium, in part, due to cellular metabolism. We then sought to examine the direct impact of adenosine and inosine. As both adenosine and inosine can enter cells via equilibrative nucleoside transporter (ENT), we examined their impact in a shorter duration of 2 h. Inosine demonstrated a more pronounced impact in upregulating PDGF-B compared to adenosine in 2 h (Figure 4G). Neither adenosine nor inosine altered the transcription of TGFβ, in keeping with a less significant impact of ADA2 on TGFβ. Furthermore, inosine also increased the transcription of ADA2 itself, whereas adenosine did not. Adenosine expectedly decreased the transcription of inflammatory cytokines such as IL1, IL10, and inosine also demonstrated a similar capacity (Figure 4G).

Paracrine impact of ADA2 stimulates the production of PDGF-B by hepatic Kupffer cells

The lack of an ortholog of human ADA2 in rodents limits *in vivo* study of ADA2 in the liver microenvironment using animal models. To examine whether ADA2 derived from infiltrative monocytes could impact Kupffer cells in a paracrine fashion in the perihepato-cellular milieu, we prepared human liver spheroids that contained cellular aggregates of hepatocytes, liver sinusoidal endothelial cells (LSEC), and Kupffer cells derived from normal human liver resections (Figure 5A). We observed significantly higher PDGF-B levels in multicellular spheroids with Kupffer cells than comparable spheroids without Kupffer cells, confirming that human hepatocytes and LSEC did not contribute significantly to the production of PDGF-B and the primary source of PDGF-B production here were Kupffer cells (Figure 5B). rhADA2 at 100 nM induced a significant upregulation of PDGF-B in Kupffer cells suggesting the biological feasibility of a paracrine loop that engages Kupffer cells in PDGF-B–mediated profibrogenic signaling (Figure 5C).

DISCUSSION

MoMF plays an essential role in the fibrogenesis in NAFLD (Ju and Tacke, 2016; Tacke and Zimmermann, 2014). This study suggests that ADA2 could be a key mediator released by MoMF that is both pro-inflammatory and pro-fibrotic (Figure 6).

Our observations suggest that infiltrative monocytes are the primary source of ADA2 in the extracellular milieu of the liver in humans. We identified a distinct population of portal macrophages that are both CD68 positive and ADA2 high, and are strongly correlated with liver fibrosis in NAFLD (Jiang et al., 2018). These cells are distinguishable from Kupffer cells by their tissue distribution, cell morphology, and cellular biomarkers. Although inflammation in nonalcoholic steatohepatitis (NASH) is generally thought to adopt a lobular pattern, portal inflammatory infiltrates, especially CD68-positive cells, are associated with liver fibrosis in NAFLD (Gadd et al., 2014). The ADA2-high portal macrophages are both CD14 and CD16 positive. The frequency of CD14/CD16-positive cells increases in the human liver with chronic disease (Liaskou et al., 2013). It has been suggested that these cells either infiltrate directly as intermediate monocytes ($CD14^+/CD16^+$) from the circulation or differentiate from classical monocytes ($CD14^+/CD16^-$) (Liaskou et al., 2013). ADA2-high portal macrophages are also positive for CCR2, CCR5, and CXCR3, suggesting that they have originated from circulating monocytes and have the capacity to migrate in response to classical monocyte chemokines: CCL2, CCL5, and CXCL10. We show that as monocytes differentiate into macrophages, they continue to express and secrete ADA2 over time *in vitro*. This biology likely occurs *in vivo* in human NAFLD. The properties of infiltrative monocyte-derived macrophages were largely defined in murine models (Ju and Tacke, 2016). Emerging studies demonstrate that resident Kupffer cells in the liver can be replaced by macrophages derived from infiltrative monocytes in murine models of NAFLD (Remmerie et al., 2020; Tran et al., 2020). To accurately define the infiltrative macrophages in humans is difficult. Validation of relevant murine macrophage markers in human NAFLD may help to determine whether this phenomena also occur in humans. The absence of an ADA2 ortholog in rodents highlights the functional differences in MoMF between mice and

humans and may contribute to the difference in the development of liver fibrosis in these two species in general.

Adenosine and ADA1 are both important factors that contribute to immune integrity. While adenosine is a potent extracellular signaling molecule, ADA1 is crucial to the viability of lymphocytes by metabolizing the toxic deoxyadenosine intracellularly (Pacheco et al., 2005). ADA1 deficiency has been associated with severe combined immunodeficiency (SCID) (Antonioli et al., 2012; Whitmore and Gaspar, 2016). Recognition of the importance of ADA2 in immune-regulation took place more recently. A burgeoning set of clinical observations has linked ADA2 deficiency with cryptic rheumatological conditions. ADA2 deficiency is now a diagnosis that accounts for a spectrum of presentations due to dysregulated immune function, including vasculopathy, cytopenia, lymphoproliferation, and polyneuropathy (Lee, 2018; Meyts and Aksentijevich, 2018). Patients with ADA2 deficiency have been shown to have constitutive activation of type I interferon (Skrabl-Baumgartner et al., 2017). A recent study by Dhanwani and colleagues indicated a deficiency of ADA2 results in the accumulation of extracellular deoxyadenosine, which in turn, leads to interferon-β-mediated inflammation (Dhanwani et al., 2020). Our study represents a scenario of increased ADA2 production, which may lead to the suppression of interferon-β production and overdrive of repair signal and fibrosis.

ADA2 is exclusively produced by monocytes, macrophages, and dendritic cells. Its circulating activity rises in conditions that classically involve macrophage engagement, such as tuberculosis and macrophage activation syndrome (Conde et al., 2002; Lee et al., 2020). Patients with type 2 diabetes, a condition often co-existing with NAFLD, can also have an increase in circulating ADA2 activity (Larijani et al., 2016). We have previously shown that high serum ADA2 activity is associated with increased stages of liver fibrosis in NAFLD (Jiang et al., 2018). *In vitro*, ADA2-stimulated macrophages demonstrate both pro-inflammatory and pro-fibrotic characteristics, a phenotype resembling M2b class, including the simultaneous upregulation of IL1, IL6, IL10, TNFα, and downregulation of CD163. The upregulation of PDGF-B has been reported in tumor-associated macrophages (TAM) to promote stroma formation (Vignaud et al., 1994). The median serum ADA2 activity in NAFLD is about 5 U/L, while patients with advanced fibrosis had serum ADA2 activities reaching 10–20 U/L (Jiang et al., 2018). In our experiments, extracellular ADA2 at 100 nM (84 U/L), significantly augmented PDGF-B production, while 10 nM ADA2 (8.4 U/L) may also have a detectable impact (Figure 3F) (Vignaud et al., 1994). Extracellular ADA2 levels in the liver lobule near the source of its production are likely to be much higher than the activity in the serum. Hence, this dose-response is physiologically relevant. Although we cannot test the *in vivo* impact of ADA2 on liver fibrosis in murine models, we did find that ADA2 promotes the production of PDGF-B in *ex vivo* human hepatic spheroids that mimic the physiological microenvironment of human hepatocytes and Kupffer cells. This indicates a paracrine loop where infiltrative monocytes magnify the pro-fibrotic signal by engaging Kupffer cells via ADA2. The biology of ADA2 in NAFLD could be relevant to the effect of Cenicriviroc, a CCR2/CCR5 antagonist that has been tested in the treatment of NASH. While Cenicriviroc inhibits the infiltration of monocytes, ADA2 modulates the impact of these cells on liver fibrosis. Interestingly, a similar paradigm has recently been observed in the brain. Zhu and colleagues showed that ADA2 promotes M2 polarization of microglia/

macrophages and mediates crosstalk between macrophages and pericytes via the paracrine activation of PDGF-BB (Zhu et al., 2017a, 2017b). Together, current evidence suggest that ADA2 impacts macrophage differentiation that may not be a binary switch. ADA2 deficiency is associated with classical macrophage differentiation potentially via a Type-I interferon response, while ADA2 over-stimulation may lead to an alternative macrophage activation, enhancing fibrosis. This response may contribute to wound healing but also cause fibrotic disease.

The molecular mechanism of ADA2 has puzzled immunologists ever since the discovery of its clinical significance. This study provided new clues and indicated some future directions. Our data suggest that ADA2 operates in part through its deaminase activity. The enzyme activity of ADA2 accounts for only one percent of ADA1 under physiological conditions (Haskó et al., 2008). Still, the presence of ADA2 significantly altered the inosine/adenosine ratio in the culture media (Figure 4F). The relevance of this deaminase activity is further supported by the loss of augmented PDGF-B production when the enzyme activity is abolished by the E359N mutation. Furthermore, inosine can increase PDGF-B transcription directly, although it does not promote a pro-inflammatory differentiation of macrophages within the 2-hour time frame. We do not know the effect of longer-term inosine exposure. As a purine metabolite, the inosine concentration in the culture media will likely decline over time, whereas ADA2, as a protein, should have a much longer half-life and could potentially maintain a sustained inosine level. The biological effect of ADA2 could in part be mediated by inosine. It is generally thought that inosine has a similar physiological impact as adenosine, although this is mostly concluded from studies with short-term stimulation (Haskó et al., 2004). The signaling mechanism of inosine has not been well studied compared to adenosine. Although some studies suggest that inosine may work through adenosine receptors (Jin et al., 1997; Tilley et al., 2000), the presence of a unique inosine receptor has not been ruled out. We found that ADA2 stimulated MoMF demonstrated upregulation of genes involved in G-protein coupled receptor and AKT-PI3P-mTOR signaling (Figures S4B–S4D). These insights may direct studies to reveal mechanisms underpinning ADA2 stimulated PDGF-B production, but not that of TGFβ. Future studies will also need to dissect the long-term versus the short-term impact of inosine and identify its signaling cascade. Furthermore, macrophages also express ADA1, an intracellular protein that can be presented on the cell surface via CD26 (Kaljas et al., 2017). Whether this occurs in the human liver and if so, how ADA2 modulates the deaminase activity of cell surface ADA1 remains to be defined. Alternatively, an inosine-independent mechanism has not been excluded. Zavialov and colleagues compared the structure of ADA1 and ADA2 and suggested that ADA2 may have an additional protein-interaction domain (Zavialov et al., 2010). Indeed, ADA2 has been shown to bind to a subset of immune cells on the surface, including regulatory T cells expressing CD39 and $CD16^{+}$ monocytes (Kaljas et al., 2017). These observations raise the possibility that ADA2 may have an undiscovered receptor that facilitates its effect. Ultimately, the role of ADA2 will need to be tested *in vivo*. ADA2 transgenic mice under a beta-actin promoter demonstrated developmental anomalies in the heart, kidney, and eyes (Riazi et al., 2005). Hence, cell-specific expression of ADA2 may be required to properly model its impact *in vivo*.

In summary, our study demonstrates that infiltrative monocytes are recruited to the liver in NAFLD and release ADA2, which in turn, promotes macrophage differentiation toward a pro-inflammatory and pro-fibrotic phenotype. These observations support further investigation of the biology of ADA2 to understand its mechanism of action in modulating inflammation and fibrosis in NAFLD.

Limitations of study

A major limitation of the current finding is the lack of *in vivo* validation. This is in part due to a lack of murine orthologs of ADA2. Future directions include the testing of ADA2 in other mammalian models or to use a humanized mouse model. Our study points to an indispensable role of the deaminase activity in the autocrine/paracrine loop, but there remain unanswered questions. On the one hand, our data cannot definitively rule out the possibility of an ADA2 receptor, whose signaling is tied to the enzyme activity. On the other, if the impact of ADA2 is completely driven by inosine, the components of the signaling cascade remains to be elucidated. This effort may lead to alternative strategies to alter the macrophages' behavior in NASH.

STAR★METHODS

RESOURCE AVAILABILITY

Lead contact—Further information and requests for resources and reagents should be directed to and will be fulfilled by the Lead Contact, Z. Gordon Jiang from Beth Israel Deaconess Medical Center, Department of Medicine, Division of Gastroenterology; zgjiang@bidmc.harvard.edu.

Materials availability—Sources of reagents and antibodies are available at the source listed above. Constructs for ADA2 are available for research purposes under an MTA, which allows the use for non-commercial purposes but not their disclosure to third parties.

Data and Code Availability

- The sequencing data are available at Gene Expression Omnibus (GEO, GSE184572). All other data are available from the Lead contact upon reasonable requests.
- This paper does not report original code.
- Any additional information required to reanalyze the data reported in this paper is available from the lead contact upon request.

EXPERIMENTAL MODEL AND SUBJECT DETAILS

Cell lines—Peripheral blood mononuclear cells (PBMCs) were obtained from anonymous healthy subjects at the Blood Donor Center at Children's Hospital (Boston, MA) by density gradient centrifugation on Ficoll-Paque (GE Healthcare). $CD14^+/CD16^+$ monocytes were isolated using a Pan Monocyte Isolation Kit (Miltenyi Biotec, Auburn, CA) according to the manufacturer's instructions. Purified $CD14^+/CD16^+$ monocytes and U937 cells were cultured in modified RPMI-1640 media containing 2 mM l-glutamine, 1.5 g/L sodium

bicarbonate, 4.5 g/L glucose, 10 mM HEPES, and 1 mM sodium pyruvate supplemented with 10% (v/v) fetal bovine serum (FBS) and 1% (v/v) penicillin/streptomycin under standard cell-culture conditions (37°C, 5% CO2, 95% humidified air). U937 cells were kindly provided by Dr. Wegiel (BIDMC, Boston, MA) and were stimulated with phorbol myristate acetate (PMA) to differentiate into macrophages. Primary $CD14^+$ / $CD16^+$ monocyte culture was supplemented with 20 ng/ml M-CSF (Peprotech, Hamburg, Germany) for 7 days to induce macrophage differentiation. CHO-K1 cells were gift from Wenda Goa and were maintained in DMEM medium supplemented with 10% (v/v) fetal bovine serum (FBS) and 1% (v/v) penicillin/streptomycin under standard cell-culture conditions.

Primary human liver tissue was obtained from surgical resection as approved by IRB protocol at Weil Cornell Medical Center. Primary human hepatocytes, liver sinusoidal endothelial cells, and human Kupffer cells were isolated as previously reported. (MacPherson et al., 2021; Song et al., 2015; Winer et al., 2020) Preparations that yielded hepatocytes with greater than 80% viability before Ficoll gradient or greater than 90% after Ficoll gradient were used for these studies.

Patient samples—Study subjects were identified from a prospective NAFLD registry at Beth Israel Deaconess Medical Center (BIDMC). Patients with a clinical diagnosis of NAFLD, subsequently confirmed by liver biopsy, were enrolled since 2009. Patients with other forms of chronic liver diseases or alternative causes for fatty liver, such as medication, hereditary hemochromatosis, or consumption of greater than 20 g alcohol daily, were excluded from the registry. Patient demographics, medical history, and physical exam findings were obtained at study enrollment. Laboratory tests and collection of serum were performed at enrollment and at follow-up visits every three months. A liver biopsy was performed on each individual within three months of the index visit. Baseline serum was stored at −80 °C. A total of 100 patients were selected from the registry to approximate a relatively equal distribution of fibrosis stages for subsequent ADA2 activity assay.(Brunt et al., 1999; Jiang et al., 2018) The mean age of the study was 56.7 ± 12.6 years and 40.7% samples were from female donors (Table 1). All patients with stage 3 and 4 fibrosis were included, while patients with stage 0, 1, and 2 fibrosis were randomly selected for inclusion. A total of 91 of 100 subjects were included in this study based on the availability of suitable liver biopsy tissues. This study has been approved by the institutional review board at BIDMC (IRB protocol 2009P000301) and was conducted in accordance with the Helsinki declaration of 1975, as revised in 1983. All subjects consented to the study at enrollment.

METHOD DETAILS

Histological staging of liver fibrosis and NASH—Ultrasound-guided liver biopsy was performed at enrollment into the study. Biopsy results were interpreted by specialized hepatobiliary pathologists. All liver biopsies were assessed and reported in a standardized fashion, including fibrosis stages (0–4) using Brunt methodology and NAFLD activity score (NAS, 0–8) using Nonalcoholic Steatohepatitis Clinical Research Network (NASH CRN) criteria calculated based on the degree of hepatic steatosis, lobular inflammation and ballooning degeneration.(Brunt et al., 1999; Kleiner et al., 2005) The diagnosis of

NASH was made based on the presence of macrovesicular steatosis in at least 5% of liver parenchyma, ballooned hepatocytes and lobular inflammation.

Histological scoring of ADA2 expression—The ADA2 immunohistochemistry of each of the 91 patients was evaluated by a hepatobiliary pathologist who provided scoring for three locations of ADA2 expression: portal tracts, lobular inflammatory foci, and Kupffer cells. Staining of macrophages in each portal tract was evaluated and assigned with a score from 0 to 3: no $ADA2^{pos}$ macrophages (score 0), 1–5 $ADA2^{pos}$ macrophages (score 1), 6–10 $ADA2^{pos}$ macrophages (score 2), and more than 10 $ADA2^{pos}$ macrophages (score 3). The average of portal tract scores was used for analysis. The score of lobular inflammatory foci was calculated by the ratio of the total number of inflammatory foci with $ADA2^{pos}$ macrophages over the total number of evaluated high power fields (HPF). The Kupffer cell staining was noted to be variable. Staining pattern was scored for intensity (0 = none, 1 = weak, 2 = moderate, 3 = strong).

Cloning, expression, and purification of wild-type and mutant ADA2—*Cecr1/Ada2* was cloned from the human cDNA library into pDirect4.0 (Antagen, Boston, MA). The E359N mutation was introduced into ADA2 by overlapping PCR. A six-histidine tag was engineered at the C-termini in both constructs. The final sequence was confirmed by DNA sequencing at Genewiz (South Plainfield, NJ). For expression, electroporation was performed to transfect ADA2 into CHO-K1 cells, followed by selection with Zeocin (400 μg/mL) for 2 weeks to establish the drug-resistant pools. The CHO cell pools were cultured in serum-free HyCell medium (GE Healthcare, Marlborough, MA) in suspension on an orbital shaker for 2–3 weeks.

rhADA2 was purified by flowing CHO cell culture media through Ni-NTA agarose (QIAGEN, Germantown, MD) in a gravity column. ADA2 on the Ni-NTA beads were washed with 20 mM imidazole in PBS and eluted with 250 mM imidazole in PBS. The elutant was dialyzed in a 30,000 kDa cutoff membrane (Millipore, Burlington, MA) against PBS at 4°C before concentrating on a 10,000 kDa Ami-con-Ultra (Millipore) device. The purity of ADA2 was confirmed by SDS-PAGE with Coomassie Blue staining. The concentration of ADA2 was determined by its deaminase activity.

Measurement of ADA2 activity—The measurement of ADA2 activity in cell culture media was performed using a commercial Adenosine Deaminase Assay kits (Diazyme, Poway, CA). The assay was based on the enzymatic deamination of adenosine to inosine which is converted to hypoxanthine by purine nucleoside phosphorylase. Hypoxanthine is then converted to uric acid and hydrogen peroxide by xanthine oxidase. Hydrogen peroxide is further reacted with N-Ethyl-N-(2-hydroxy-3-sulfopropyl)-3-methylaniline and 4-aminoantipyrine in the presence of peroxidase to generate quinone dye, which was monitored on a SpectroMax M5 spectrometer at 550 nm wavelength. The measurement of ADA2 activity was conducted in the presence of erythro-9-(2-hydroxy-3-nonyl) adenine (EHNA), an ADA1-specific inhibitor. The test was validated using ADA control and calibrators (Diazyme) and performed following the manufacturer's instructions.

Measurement of adenosine and inosine concentration—The measurement of adenosine and inosine concentration was conducted using the Adenosine Assay Kit (Abcam, ab211094) and Inosine Assay Kit (Abcam, ab126286) respectively. Similar principal was adopted in both assay kits. A fluorometric indicator was used to measure the concentration of a product converted from either adenosine or inosine. The adensoine and inosine concentration was calculated based on the measurement in the presenece or absence of the enzymatic converter. Culture media were harvested and stored at −80 C prior to the assay. Upon thawing, the media was diluated 5x before analysis referenced against internal standards of adenosine and inosine respectively.

Immunostaining—Formalin-fixed, paraffin-embedded (FFPE) human liver tissues were cut into 5 μm sections. For immunohistochemistry, sections were blocked with 7% horse serum (Vector Labs, Burlingame, CA) for half an hour, and incubated with primary antibody overnight at 4°C (Table S1). The sections were then blocked against peroxidase and biotin activity, incubated with biotinylated secondary antibody for one hour, and then treated with horseradish peroxidase (HRP) conjugated avidin (Vector Labs, Burlingame, CA) to visualize with ImmPACT DAB (Vector Labs). All slides were mounted on Cytoseal, examined and recorded on a Nikon microscope. For immunofluorescent staining, we used the respective fluorescent secondary antibodies, or streptavidin conjugated with Alexa Fluor 594 (Jackson ImmunoResearch, West Grove, PA). Sections were co-stained with Hoechst and covered with polyvinyl alcohol mounting medium (Sigma-Aldrich) and examined on a Nikon Multi-Photon Fluorescent Microscope.

Flow Cytometry—ADA2 expression on monocytes was determined by Flow Cytometry. Peripheral blood-derived cells were permeabilized and incubated with rabbit against human ADA2 antibody (Novus Cat #NBP1-89238, Centennial, CO) followed by donkey anti-rabbit Alexa647 antibody (Biolegend, San Diego, CA) (Table S1). Additionally, CD14- APC/Cy7 and CD16-PB were used to stain monocytes. Cells were acquired on Cytoflex LX II (Beckman Coulter, Chaska, Minnesota) and analyzed on CytExpert Analysis Software v2 (Beckman Coulter, Chaska, Minnesota).

RNA *in situ* hybridization—RNA *in situ* hybridization (ISH) was performed with the RNAScope Red Manual Assay 2.5 Kit (ACDBio, Newark, CA). The Hs-CECR1 probe was designed by ACDBio according to the standard *in silico* algorithm to ensure target specificity. FFPE liver biopsy sections were first de-paraffinized using xylene and ethanol, and incubated in the pretreatment buffer with protease and incubated in a HybEZ oven (ACDBio) to expose mRNA. The staining of mRNA was achieved by hybridization with the target Hs-CECR1 probe over the pretreated liver tissue, followed by sequential treatment of amplification reagents provided in the RNAScope kit. Hematoxylin was used as a nuclear counterstain. Each section was dehydrated before being mounted with Pertex (ACDBio). A probe against a housekeeping gene *PPIB* was used as a positive control (ACDBio).

Real-time PCR—Gene transcription was analyzed in U937 differentiated macrophages and human monocyte derived macrophages after 48 hours of stimulation with 100 nM wild-type or mutant recombinant human ADA2 (rhADA2), or at concentrations otherwise

indicated. Cells were treated with 100 μM adenosine or inosine for 2 hours and harvested for transcription analysis. Culture media were collected for protein analysis. Total RNA was extracted cells using the Trizol method and concentration was measured on Nanodrop ND 1000 spectrophotometer (Wilmington, DE, USA). Reverse transcription was performed on 1 g of total RNA using iScript cDNA Synthesis Kit (BioRad, Hercules, CA).

RNaseq—Total RNA was extracted and purified from cells using RNeasy Kit (QIAGEN) according to the manufacturer's instructions prior to RNaseq at Genewiz. RNA concentration was determined with Qubit™ RNA Assay (Thermo Fischer, Waltham, MA) and measured on the TapeStation System. RNA library preparation was performed using a polyA selection method. RNA sequencing was performed using the Illumina HiSeq system in a 2 × 150-bp configuration with single index per lane). Sequence reads were trimmed to remove possible adaptor sequences and nucleotides with poor quality using Trimmomatic v.0.36. The trimmed reads were mapped to the *Homo sapiens* GRCh38 reference genome available on ENSEMBL using the STAR aligner v.2.5.2b. Using DESeq2, a comparison of gene expression between the customer-defined groups of samples was performed. The Wald test was used to generate p values and log2 fold changes. Further analysis was carried out using the ClusterProfiler package by R (v.3.6.0).(Yu et al., 2012) GSEA was performed by using the GSEA-P software, MSigDB database v7.1 as described previously.(Subramanian et al., 2005)

Measurement of PDGF-BB concentration—PDGF-BB concentration in the culture media was dilated five-fold and measured using Human PDGF-BB ELISA Kit (Millipore Sigma, RAB0397) according to the manufacturer's protocol.

Western blot—Cells lysates were collected in ice-cold RIPA Buffer (ThermoFisher) supplemented with Protease Inhibitor Cocktail (ThermoFisher). Total protein concentration was quantified with Bio-Rad DC protein assay reagent (Bio-Rad) using bovine serum albumin as the standard. Cell lysate or culture media was mixed in 5x XT sample buffer (Bio-Rad) and denatured at 95°C for 5 min to prepare the gel sample and loaded on 4%–12% Criterion XT Bis-Tris SDS-PAGE gels (Bio-Rad). The gel was transferred onto PVDF membrane (Millipore) on a Trans-Blot semi-dry transfer cell (Bio-Rad). Immunoblot was first blocked with Odyssey Blocking buffer (Li-Cor, Lincoln, ME), followed by incubation with rabbit anti-CERC1 (Novus Cat #NBP1-89238, Centennial, CO), rabbit anti-human PDGF-BB antibody (Abcam), Erk1/2 (Cell Signaling, Danvers, MA), or mouse anti-β-actin antibodies (Abcam), and detected with IRDye 800CW Goat anti-Rabbit (Li-Cor) or IRDye 680RD Donkey anti-Mouse (Li-Cor) secondary antibodies on the Odyssey scanner (LI-Cor).

Human hepatic multicellular spheroids preparation—The generation of multicellular spheroids and their applications have been described previously.(MacPherson et al., 2021; Song et al., 2015; Winer et al., 2020) Briefly, polydimethylsiloxane (PDMS) microwells were fabricated using standard soft lithography at the Cornell NanoScale Facility (CNF). Briefly, the photomask with micropatterns was prepared using a mask writer (DWL2000, Heidelberg Instruments, Heidelberg, Germany). The silicon wafer was spin-coated with SU-8 2150 photoresist (Micro-Chem, Westborough, MA) at 500 rpm for 40

s and then 2500 rpm for 30 s. The wafer was covered with the photomask and exposed with a UV photolithography machine (ABM Contact Aligner) for 32 s. After being developed and post-baked, the SU-8 master wafer was fabricated. The master wafer has microposts with various diameters and thickness of 220 μm. The master wafer was then used to create PDMS (Sylgard 184, Dow Corning) microwells. A mixture (10:1, w-w) of Sylgard 184 silicone elastomer components was casted onto the master wafer, cured at 60°C overnight, and peeled off from master to obtain PDMS microwells. PDMS microwells hole-punched to fit the well dimension of 24-well plate. The hole-punched PDMS microwells were then adhered to wells of 24-well plate. Immediately before usage, the 24 well plate with microwells were sterilized with UV treatment for 30min. 1% (w/v) Pluronic® F127 (Sigma) solution was added into each well and spun at 2000 rpm. The wells were incubated at room temperature for 1 hr to enable Pluronic to coat the PDMS surface to prevent cell attachment on PDMS surface and facilitate the formation of cell aggregates.

To form cell aggregates, cell suspensions of primary human hepatocytes (1.8×10^5 cells) and human liver sinusoidal endothelial cells (at a ratio of 5:1) were added to each well of a 24-well plate with PDMS microwells inside. For cultures, primary human hepatocytes, human liver sinusoidal endothelial cells, and Kupffer cells were mixed at a ratio of 10:2:1 and spun down at 50 g for 5 min to allow cells to sink to the microwells. The cells that fell into the microwells formed cell aggregates after overnight culture with gentle shaking. The cell aggregates were cultured in microwells for 7 days before initiating experiments. Cells were cultured in Dulbecco Modified Eagle Media with high glucose, 10% FBS, 1% insulin, transferrin, selenous acid premix (BD Biosciences, Bedford, MA), glucagon 7 ng/mL, dexamethasone 40 ng/mL, and 1% penicillin-streptomycin. Media was changed every two days unless as needed for experiments.

Stimulation by rhADA2 was conducted by incubating spheroids either with or without Kupffer cells in the presence of 100 nM rhADA2 or controls. The spheroids were harvested after 48 hours to isolate mRNA for real-time PCR quantitation of PDGF-B.

Graphical rendering of ADA2—The crystal structure of ADA2 was previously described and retrieved from the protein data bank (PDB ID: Q9NZK5).(Zavialov et al., 2010) The structure of ADA2 dimer was rendered in a hybrid wire and ribbon diagrams using MOLMOL.(Koradi et al., 1996)

QUANTIFICATION AND STATISTICAL ANALYSIS

To investigate the relationship between $ADA2^{pos}$ cells and histological scores of NAFLD, we performed linear regression using the scores of $ADA2^{pos}$ portal macrophages, Kupffer cells and cells in inflammatory foci as dependent variables and fibrosis stage, histological scores of lobular inflammation and ballooning degeneration as independent variables using Stata (StataCorp, College Station, Texas). Comparisons among groups elsewhere were conducted by a two-tailed Student’s t test for two-group comparison or ANOVA for comparison of three or more groups using Prism (GraphPad, San Diego, CA). Normal distribution was confirmed for dependent variables in the regression analysis and all groups for t test and ANOVA.

Supplementary Material

Refer to Web version on PubMed Central for supplementary material.

ACKNOWLEDGMENTS

This work is in part supported by a grant by the German Research Foundation (DFG) to S.T.H. (DFG TI-988/1-1), the Clinical Research Award from the American College of Gastroenterology to Z.G.J., the Alan Hofmann Clinical and Translational Research Award from the American Associations for the Study of Liver Diseases (AASLD) to Z.G.J., the Irma Hirschl Trust Research Scholar Award to R.E.S., and National Institute of Health (NIH) grants to S.C.R. (P01HL107152, R21CA164970), Z.G.J. (K08DK115883), M.L. (K23DK083439), and R.E.S. (R01CA234614, R01AI107301, R01DK121072, R01AA027327).

REFERENCES

Adams LA, Lymp JF, St Sauver J, Sanderson SO, Lindor KD, Feldstein A, and Angulo P (2005). The natural history of nonalcoholic fatty liver disease: a population-based cohort study. J. Gastro 129, 113–121. 10.1053/j.gastro.2005.04.014.

Angulo P, Kleiner DE, Dam-Larsen S, Adams LA, Bjornsson ES, Charatcharoenwitthaya P, Mills PR, Keach JC, Lafferty HD, Stahler A, et al. (2015). Liver Fibrosis, but No Other Histologic Features, Is Associated With Long-term Outcomes of Patients With Nonalcoholic Fatty Liver Disease. Gastroenterology 149, 389, 97.e10. 10.1053/j.gastro.2015.04.043. [PubMed: 25935633]

Antonioli L, Colucci R, La Motta C, Tuccori M, Awwad O, Da Settimo F, Blandizzi C, and Fornai M (2012). Adenosine deaminase in the modulation of immune system and its potential as a novel target for treatment of inflammatory disorders. Curr. Drug Targets 13, 842–862. [PubMed: 22250650]

Antonioli L, Pacher P, Vizi ES, and Haskó G (2013). CD39 and CD73 in immunity and inflammation. Trends Mol. Med 19, 355–367. 10.1016/j.molmed.2013.03.005. [PubMed: 23601906]

Baeck C, Wehr A, Karlmark KR, Heymann F, Vucur M, Gassler N, Huss S, Klussmann S, Eulberg D, Luedde T, et al. (2012). Pharmacological inhibition of the chemokine CCL2 (MCP-1) diminishes liver macrophage infiltration and steatohepatitis in chronic hepatic injury. Gut 61, 416–426. 10.1136/gutjnl-2011-300304. [PubMed: 21813474]

Browning JD, Szczepaniak LS, Dobbins R, Nuremberg P, Horton JD, Cohen JC, Grundy SM, and Hobbs HH (2004). Prevalence of hepatic steatosis in an urban population in the United States: impact of ethnicity. Hepatology 40, 1387–1395. 10.1002/hep.20466. [PubMed: 15565570]

Brunt EM, Janney CG, Di Bisceglie AM, Neuschwander-Tetri BA, and Bacon BR (1999). Nonalcoholic steatohepatitis: a proposal for grading and staging the histological lesions. Am. J. Gastroenterol 94, 2467–2474. 10.1111/j.1572-0241.1999.01377.x. [PubMed: 10484010]

Conde MB, Marinho SR, Pereira Mde.F., Lapa e Silva JR, Saad MH, Sales CL, Ho JL, and Kritski AL (2002). The usefulness of serum adenosine deaminase 2 (ADA2) activity in adults for the diagnosis of pulmonary tuberculosis. Respir. Med 96, 607–610. 10.1053/rmed.2001.1273. [PubMed: 12206153]

Deaglio S, and Robson SC (2011). Ectonucleotidases as regulators of purinergic signaling in thrombosis, inflammation, and immunity. Adv. Pharmacol 61, 301–332. 10.1016/B978-0-12-385526-8.00010-2. [PubMed: 21586363]

Dhanwani R, Takahashi M, Mathews IT, Lenzi C, Romanov A, Watrous JD, Pieters B, Hedrick CC, Benedict CA, Linden J, et al. (2020). Cellular sensing of extracellular purine nucleosides triggers an innate IFN-β response. Sci. Adv 6, eaba3688. 10.1126/sciadv.aba3688. [PubMed: 32743071]

Dranoff JA, Feld JJ, Lavoie EG, and Fausther M (2014). How does coffee prevent liver fibrosis? Biological plausibility for recent epidemiological observations. Hepatology 60, 464–467. 10.1002/hep.27032. [PubMed: 24464631]

Ekstedt M, Hagström H, Nasr P, Fredrikson M, Stål P, Kechagias S, and Hultcrantz R (2015). Fibrosis stage is the strongest predictor for disease-specific mortality in NAFLD after up to 33 years of follow-up. Hepatology 61, 1547–1554. 10.1002/hep.27368. [PubMed: 25125077]

Eltzschig HK, Sitkovsky MV, and Robson SC (2012). Purinergic signaling during inflammation. N. Engl. J. Med 367, 2322–2333. 10.1056/NEJMra1205750. [PubMed: 23234515]

Fausther M (2018). Extracellular adenosine: a critical signal in liver fibrosis. Am. J. Physiol. Gastrointest. Liver Physiol 315, G12–G19. 10.1152/ajpgi.00006.2018.

Friedman SL (2013). Liver fibrosis in 2012: Convergent pathways that cause hepatic fibrosis in NASH. Nat. Rev. Gastroenterol. Hepatol 10, 71–72. 10.1038/nrgastro.2012.256. [PubMed: 23296246]

Gadd VL, Skoien R, Powell EE, Fagan KJ, Winterford C, Horsfall L, Irvine K, and Clouston AD (2014). The portal inflammatory infiltrate and ductular reaction in human nonalcoholic fatty liver disease. Hepatology 59, 1393–1405. 10.1002/hep.26937. [PubMed: 24254368]

Haskó G, Sitkovsky MV, and Szabó C (2004). Immunomodulatory and neuroprotective effects of inosine. Trends Pharmacol. Sci 25, 152–157. 10.1016/j.tips.2004.01.006. [PubMed: 15019271]

Haskó G, Linden J, Cronstein B, and Pacher P (2008). Adenosine receptors: Therapeutic aspects for inflammatory and immune diseases. Nat. Rev. Drug Discov 7, 759–770. 10.1038/nrd2638. [PubMed: 18758473]

Jiang ZG, Sandhu B, Feldbrügge L, Yee EU, Csizmadia E, Mitsuhashi S, Huang J, Afdhal NH, Robson SC, and Lai M (2018). Serum activity of macrophage-derived adenosine deaminase 2 is associated with liver fibrosis in nonalcoholic fatty liver disease. Clin. Gastroenterol. Hepatol 16, 1170–1172. 10.1016/j.cgh.2017.11.028. [PubMed: 29170098]

Jin X, Shepherd RK, Duling BR, and Linden J (1997). Inosine binds to A3 adenosine receptors and stimulates mast cell degranulation. J. Clin. Invest 100, 2849–2857. 10.1172/JCI119833. [PubMed: 9389751]

Ju C, and Tacke F (2016). Hepatic macrophages in homeostasis and liver diseases: from pathogenesis to novel therapeutic strategies. Cell. Mol. Immunol 13, 316–327. 10.1038/cmi.2015.104. [PubMed: 26908374]

Kaljas Y, Liu C, Skaldin M, Wu C, Zhou Q, Lu Y, Aksentijevich I, and Zavialov AV (2017). Human adenosine deaminases ADA1 and ADA2 bind to different subsets of immune cells. Cell. Mol. Life Sci 74, 555–570. 10.1007/s00018-016-2357-0. [PubMed: 27663683]

Karlmark KR, Weiskirchen R, Zimmermann HW, Gassler N, Ginhoux F, Weber C, Merad M, Luedde T, Trautwein C, and Tacke F (2009). Hepatic recruitment of the inflammatory Gr1+ monocyte subset upon liver injury promotes hepatic fibrosis. Hepatology 50, 261–274. 10.1002/hep.22950. [PubMed: 19554540]

Kleiner DE, Brunt EM, Van Natta M, Behling C, Contos MJ, Cummings OW, Ferrell LD, Liu YC, Torbenson MS, Unalp-Arida A, et al. ; Nonalcoholic Steatohepatitis Clinical Research Network (2005). Design and validation of a histological scoring system for nonalcoholic fatty liver disease. Hepatology 41, 1313–1321. 10.1002/hep.20701. [PubMed: 15915461]

Koradi R, Billeter M, and Wuthrich K (1996). MOLMOL: a program for display and analysis of macromolecular structures. J Mol Graph 14, 51–55, 29–32. [PubMed: 8744573]

Krenkel O, Puengel T, Govaere O, Abdallah AT, Mossanen JC, Kohlhepp M, Liepelt A, Lefebvre E, Luedde T, Hellerbrand C, et al. (2018). Therapeutic inhibition of inflammatory monocyte recruitment reduces steatohepatitis and liver fibrosis. Hepatology 67, 1270–1283. 10.1002/hep.29544. [PubMed: 28940700]

Kruger AJ, Fuchs BC, Masia R, Holmes JA, Salloum S, Sojoodi M, Ferreira DS, Rutledge SM, Caravan P, Alatrakchi N, et al. (2018). Prolonged cenicriviroc therapy reduces hepatic fibrosis despite steatohepatitis in a diet-induced mouse model of nonalcoholic steatohepatitis. Hepatol. Commun 2, 529–545. 10.1002/hep4.1160. [PubMed: 29761169]

Larijani B, Heshmat R, Ebrahimi-Rad M, Khatami S, Valadbeigi S, and Saghiri R (2016). Diagnostic value of adenosine deaminase and its isoforms in type II diabetes mellitus. Enzyme Res. 2016, 9526593. 10.1155/2016/9526593. [PubMed: 28050278]

Lee PY (2018). Vasculopathy, immunodeficiency, and bone marrow failure: The intriguing syndrome caused by deficiency of adenosine deaminase 2. Front Pediatr. 6, 282. 10.3389/fped.2018.00282. [PubMed: 30406060]

Lee PY, Schulert GS, Canna SW, Huang Y, Sundel J, Li Y, Hoyt KJ, Blaustein RB, Wactor A, Do T, et al. (2020). Adenosine deaminase 2 as a biomarker of macrophage activation syndrome in systemic juvenile idiopathic arthritis. Ann. Rheum. Dis 10.1136/annrheumdis-2019-216030.

Liaskou E, Zimmermann HW, Li KK, Oo YH, Suresh S, Stamataki Z, Qureshi O, Lalor PF, Shaw J, Syn WK, et al. (2013). Monocyte subsets in human liver disease show distinct phenotypic and functional characteristics. Hepatology 57, 385–398. 10.1002/hep.26016. [PubMed: 22911542]

MacParland SA, Liu JC, Ma XZ, Innes BT, Bartczak AM, Gage BK, Manuel J, Khuu N, Echeverri J, Linares I, et al. (2018). Single cell RNA sequencing of human liver reveals distinct intrahepatic macrophage populations. Nat. Commun 9, 4383. 10.1038/s41467-018-06318-7. [PubMed: 30348985]

MacPherson D, Bram Y, Park J, and Schwartz RE (2021). Peptide-based scaffolds for the culture and maintenance of primary human hepatocytes. Sci. Rep 11, 6772. 10.1038/s41598-021-86016-5. [PubMed: 33762604]

Meyts I, and Aksentijevich I (2018). Deficiency of adenosine deaminase 2 (DADA2): Updates on the phenotype, genetics, pathogenesis, and t5reatment. J. Clin. Immunol 38, 569–578. 10.1007/s10875-018-0525-8. [PubMed: 29951947]

Miura K, Yang L, van Rooijen N, Ohnishi H, and Seki E (2012). Hepatic recruitment of macrophages promotes nonalcoholic steatohepatitis through CCR2. Am. J. Physiol. Gastrointest. Liver Physiol 302, G1310–G1321. 10.1152/ajpgi.00365.2011. [PubMed: 22442158]

Navon Elkan P, Pierce SB, Segel R, Walsh T, Barash J, Padeh S, Zlotogorski A, Berkun Y, Press JJ, Mukamel M, et al. (2014). Mutant adenosine deaminase 2 in a polyarteritis nodosa vasculopathy. N. Engl. J. Med 370, 921–931. 10.1056/NEJMoa1307362. [PubMed: 24552285]

Pacheco R, Martinez-Navio JM, Lejeune M, Climent N, Oliva H, Gatell JM, Gallart T, Mallol J, Lluis C, and Franco R (2005). CD26, adenosine deaminase, and adenosine receptors mediate costimulatory signals in the immunological synapse. Proc. Natl. Acad. Sci. USA 102, 9583–9588. 10.1073/pnas.0501050102. [PubMed: 15983379]

Remmerie A, Martens L, Thoné T, Castoldi A, Seurinck R, Pavie B, Roels J, Vanneste B, De Prijck S, Vanhockerhout M, et al. (2020). Osteopontin expression identifies a subset of recruited macrophages distinct from Kupffer cells in the fatty liver. Immunity 53, 641–657.e14. 10.1016/j.immuni.2020.08.004. [PubMed: 32888418]

Riazi AM, Van Arsdell G, and Buchwald M (2005). Transgenic expression of CECR1 adenosine deaminase in mice results in abnormal development of heart and kidney. Transgenic Res. 14, 333–336. [PubMed: 16145841]

Saab S, Mallam D, Cox GA 2nd, and Tong MJ (2014). Impact of coffee on liver diseases: A systematic review. Liver Int. 34, 495–504. 10.1111/liv.12304. [PubMed: 24102757]

Skrabl-Baumgartner A, Plecko B, Schmidt WM, König N, Hershfield M, Gruber-Sedlmayr U, and Lee-Kirsch MA (2017). Autoimmune phenotype with type I interferon signature in two brothers with ADA2 deficiency carrying a novel CECR1 mutation. Pediatr. Rheumatol. Online J 15, 67. 10.1186/s12969-017-0193-x. [PubMed: 28830446]

Song W, Lu YC, Frankel AS, An D, Schwartz RE, and Ma M (2015). Engraftment of human induced pluripotent stem cell-derived hepatocytes in immunocompetent mice via 3D co-aggregation and encapsulation. Sci. Rep 5, 16884. 10.1038/srep16884. [PubMed: 26592180]

Subramanian A, Tamayo P, Mootha VK, Mukherjee S, Ebert BL, Gillette MA, Paulovich A, Pomeroy SL, Golub TR, Lander ES, and Mesirov JP (2005). Gene set enrichment analysis: a knowledge-based approach for interpreting genome-wide expression profiles. Proc. Natl. Acad. Sci. USA 102, 15545–15550. 10.1073/pnas.0506580102. [PubMed: 16199517]

Tacke F, and Zimmermann HW (2014). Macrophage heterogeneity in liver injury and fibrosis. J. Hepatol 60, 1090–1096. 10.1016/j.jhep.2013.12.025. [PubMed: 24412603]

Tilley SL, Wagoner VA, Salvatore CA, Jacobson MA, and Koller BH (2000). Adenosine and inosine increase cutaneous vasopermeability by activating A(3) receptors on mast cells. J. Clin. Invest 105, 361–367. 10.1172/JCI8253. [PubMed: 10675362]

Tran S, Baba I, Poupel L, Dussaud S, Moreau M, Gélineau A, Marcelin G, Magréau-Davy E, Ouhachi M, Lesnik P, et al. (2020). Impaired Kupffer cell self-renewal alters the liver response to lipid overload during non-alcoholic steatohepatitis. Immunity 53, 627–640.e5. 10.1016/j.immuni.2020.06.003. [PubMed: 32562600]

Vignaud JM, Marie B, Klein N, Plénat F, Pech M, Borrelly J, Martinet N, Duprez A, and Martinet Y (1994). The role of platelet-derived growth factor production by tumor-associated macrophages in tumor stroma formation in lung cancer. Cancer Res. 54, 5455–5463. [PubMed: 7923179]

Whitmore KV, and Gaspar HB (2016). Adenosine deaminase deficiency—More than just an immunodeficiency. Front. Immunol 7, 314. 10.3389/fimmu.2016.00314. [PubMed: 27579027]

Winer BY, Gaska JM, Lipkowitz G, Bram Y, Parekh A, Parsons L, Leach R, Jindal R, Cho CH, Shrirao A, et al. (2020). Analysis of host responses to hepatitis B and delta viral infections in a micro-scalable hepatic co-culture system. Hepatology 71, 14–30. 10.1002/hep.30815. [PubMed: 31206195]

Younossi ZM, Koenig AB, Abdelatif D, Fazel Y, Henry L, and Wymer M (2016). Global epidemiology of nonalcoholic fatty liver disease—Meta-analytic assessment of prevalence, incidence, and outcomes. Hepatology 64, 73–84. 10.1002/hep.28431. [PubMed: 26707365]

Yu G, Wang LG, Han Y, and He QY (2012). clusterProfiler: An R package for comparing biological themes among gene clusters. OMICS 16, 284–287. 10.1089/omi.2011.0118. [PubMed: 22455463]

Zavialov AV, and Engström A (2005). Human ADA2 belongs to a new family of growth factors with adenosine deaminase activity. Biochem. J 391, 51–57. 10.1042/BJ20050683. [PubMed: 15926889]

Zavialov AV, Yu X, Spillmann D, Lauvau G, and Zavialov AV (2010). Structural basis for the growth factor activity of human adenosine deaminase ADA2. J. Biol. Chem 285, 12367–12377. 10.1074/jbc.M109.083527. [PubMed: 20147294]

Zhang X, Shen J, Man K, Chu ES, Yau TO, Sung JC, Go MY, Deng J, Lu L, Wong VW, et al. (2014). CXCL10 plays a key role as an inflammatory mediator and a non-invasive biomarker of non-alcoholic steatohepatitis. J. Hepatol 61, 1365–1375. 10.1016/j.jhep.2014.07.006. [PubMed: 25048951]

Zhou Q, Yang D, Ombrello AK, Zavialov AV, Toro C, Zavialov AV, Stone DL, Chae JJ, Rosenzweig SD, Bishop K, et al. (2014). Early-onset stroke and vasculopathy associated with mutations in ADA2. N. Engl. J. Med 370, 911–920. 10.1056/NEJMoa1307361. [PubMed: 24552284]

Zhu C, Chrifi I, Mustafa D, van der Weiden M, Leenen PJM, Duncker DJ, Kros JM, and Cheng C (2017a). CECR1-mediated cross talk between macrophages and vascular mural cells promotes neovascularization in malignant glioma. Oncogene 36, 5356–5368. 10.1038/onc.2017.145. [PubMed: 28534507]

Zhu C, Mustafa D, Zheng PP, van der Weiden M, Sacchetti A, Brandt M, Chrifi I, Tempel D, Leenen PJM, Duncker DJ, et al. (2017b). Activation of CECR1 in M2-like TAMs promotes paracrine stimulation-mediated glial tumor progression. Neuro-oncol. 19, 648–659. 10.1093/neuonc/now251. [PubMed: 28453746]

Zimmermann HW, Seidler S, Nattermann J, Gassler N, Hellerbrand C, Zernecke A, Tischendorf JJ, Luedde T, Weiskirchen R, Trautwein C, and Tacke F (2010). Functional contribution of elevated circulating and hepatic non-classical CD14CD16 monocytes to inflammation and human liver fibrosis. PLoS ONE 5, e11049. 10.1371/journal.pone.0011049. [PubMed: 20548789]

Highlights

- NAFLD fibrosis is associated with an accumulation of ADA2-positive portal macrophages
- Infiltrative monocytes in the liver produce ADA2 upon differentiation
- ADA2 promotes a pro-inflammatory and pro-fibrotic differentiation of liver macrophages
- ADA2 induces the release of PDGF-B from monocyte-derived macrophages and Kupffer cells

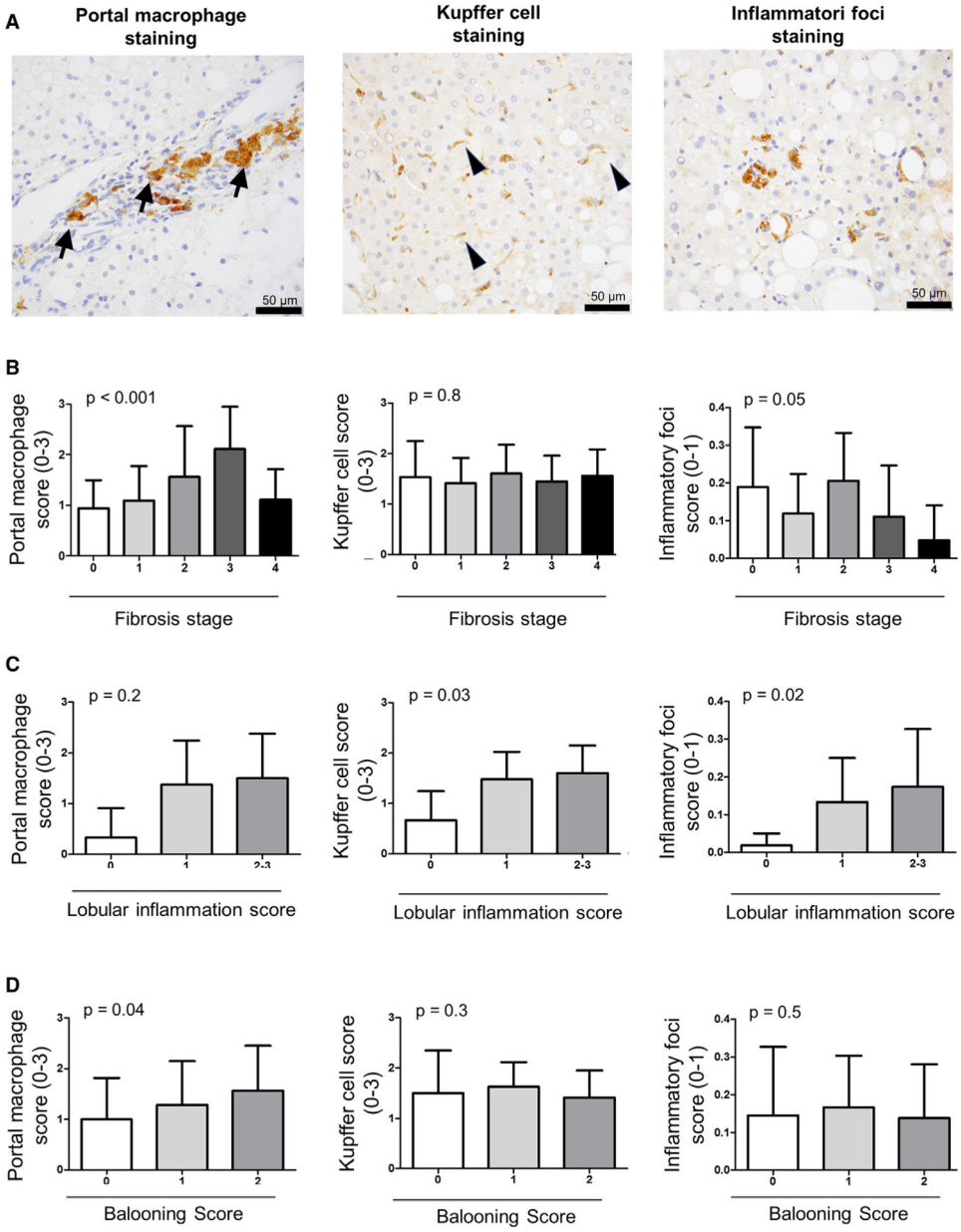

Figure 1. Portal macrophages are associated with liver fibrosis in NAFLD

(A) Three patterns of ADA2^{pos} cells in NAFLD by immunohistochemistry (IHC) of liver biopsies: portal macrophages, Kupffer cells, and mononuclear cells in inflammatory foci. Representative images were taken from 91 liver biopsies. Arrows indicate portal macrophages with intense staining of ADA2. Arrowheads show spindle-shaped Kupffer cells. Scale bar representing 50 µm.

(B) Relationship between liver fibrosis and IHC scores of ADA2^{pos} portal macrophages, Kupffer cells, and inflammatory foci.

(C) Relationship between lobular inflammation score (0–3) and IHC scores of ADA2^{pos} portal macrophages, Kupffer cells, and inflammatory foci.

(D) Relationship between ballooning degeneration score (0–2) and IHC scores of ADA2^{pos} portal macrophages, Kupffer cells, and inflammatory foci.
(B–D) Error bars represent standard deviation; p value calculated by linear regression.

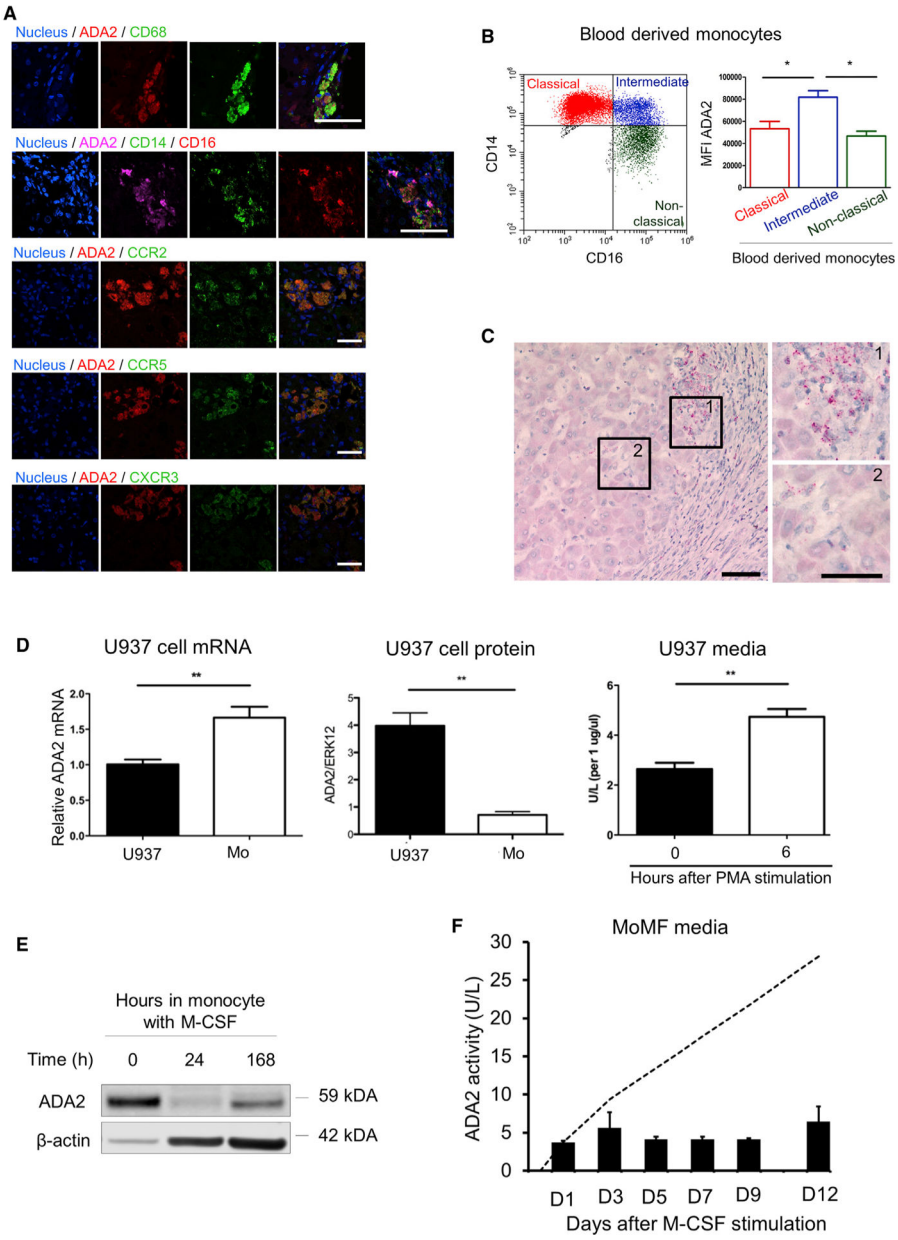

Figure 2. Intermediate monocytes release ADA2 upon differentiation into macrophages

(A) Fluorescent immunomicroscopy of ADA2 and macrophage markers in the portal area. Serial sections are used for CCR2, CCR5 and CXCR3 stains to highlight co-localization. Scale bar represents 50 μm.

(B) Flow cytometry of CD14+/CD16+ monocytes showing the distribution of classical, intermediate, and nonclassical monocytes from peripheral blood and expression of ADA2 measured by mean fluorescent index.

(C) *In situ* hybridization (ISH) of ADA2 mRNA by RNAscope of a liver biopsy with cirrhosis. Enlarged views of an inflammatory focus and lobular area are shown on the right. Scale bar represents 50 μm.

(D) The mRNA and protein levels of ADA2 in U937 cells and activity in the culture media upon PMA induced macrophage differentiation. Cells or culture media 6 h after PMA induction were collected. ADA2 mRNA was measured by qPCR. ADA2 protein level was measured by the relative intensity of ADA2 and ERK1, a control protein, on western blot.
(E) Western blot demonstrating changes in ADA2 protein levels in human monocyte derived macrophages. Cells were analyzed at 0, 24, and 168 h after M-CSF induced differentiation. Sample loading normalized by total protein.
(F) Activity of ADA2 in the culture media of MoMF induced by M-CSF (n = 2). Media was collected and replaced on day 1, 3, 5, 7, 9, 12. The dashed line represents the estimated accumulative ADA2 activity had media not been replaced. Error bars represent standard deviation.

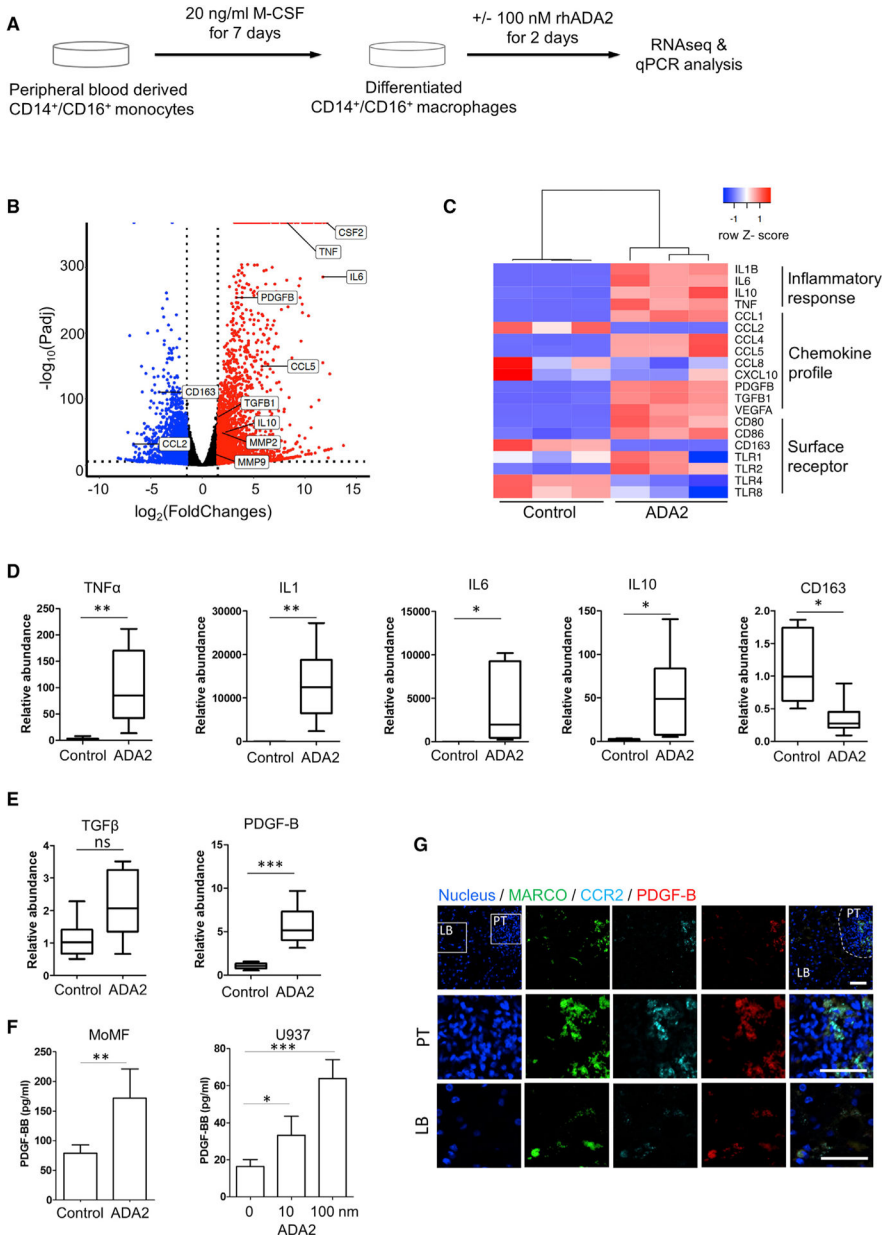

Figure 3. ADA2 promotes a pro-inflammatory and pro-fibrotic differentiation of macrophages

(A) A diagram of the experiment setup.

(B) A volcano plot of the changes of gene transcription in response to ADA2 in comparison to PBS (n = 3 in each group). Dotted lines mark 1.5 log2fold changes and p values at 0.001.

(C) Heatmap of representative genes for macrophage phenotypes.

(D and E) Validation of pro-inflammatory (D) and pro-fibrotic (E) gene regulations in response to ADA2 in comparison to PBS. Human monocyte derived macrophages (MoMF) (n = 6, different individuals) are used in the assay. Box and Whisker plots with two-tailed t tests are used to calculate p values.

(F) PDGF-BB release from MoMF and U937 cells in response to ADA2. PDGF-BB concentration measured by ELISA in the culture media (n = 6). p value calculated by t

test for MoMF and one-way ANOVA for U937 cells. Error bars represent standard deviation. *p < 0.05; **p < 0.01; ***p < 0.001.

(G) Immunofluorescent costaining of MARCO, CCR2 and PDGF-B. Dashed line demarcatse portal triad (PT) and lobular regions (LB) in the first row. Enlarged areas of PT and LB (square box) are shown in 2nd and 3rd rows. Scale bars represent 50 μm.

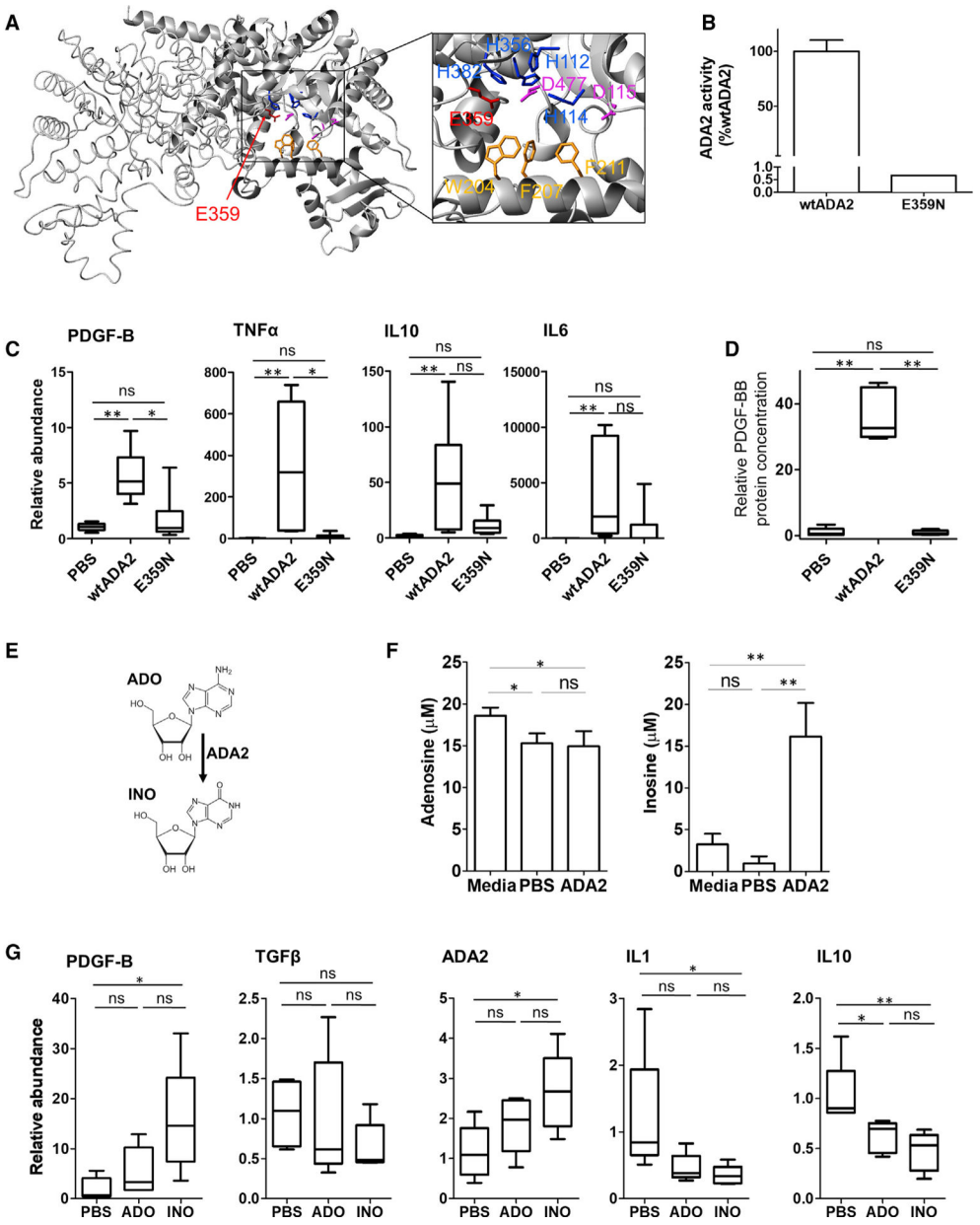

Figure 4. Deaminase activity of ADA2 contributes to the impact of ADA2 on PDGF-B production

(A) The 3D structure of ADA2 (PDB ID: 3lgd). One molecule in the ADA2 dimer is shown in a ribbon diagram with its active site shown in an enlarged box with key residues in highlights.

(B) A comparison of deaminase activity between wild-type ADA2 (wtADA2) and E359N mutant.

(C) Comparisons of transcriptional responses to wtADA2 and E359N in human monocyte derived macrophages (MoMF) (n = 6).

(D) A comparison of PDGF-BB production in response to wtADA2 and E359N. Fluorescent signal measured from western blot normalized to PBS.

(E) A diagram of the conversion from adenosine (ADO) to inosine (INO) by ADA2.

(F) Comparisons of adenosine, inosine concentrations in the cell free RPMI media, control MoMF, and MoMF after wtADA2 stimulation.
(G) Comparisons on transcriptional responses to adenosine and inosine in human monocyte derived macrophages (n = 6). p values calculated from one-way ANOVA in (C), (D), (F), and (G). Error bars represent standard deviation in (B) and (F). Box and Whisker plots in (C), (D), and (F). *p < 0.05; **p < 0.01; ***p < 0.001.

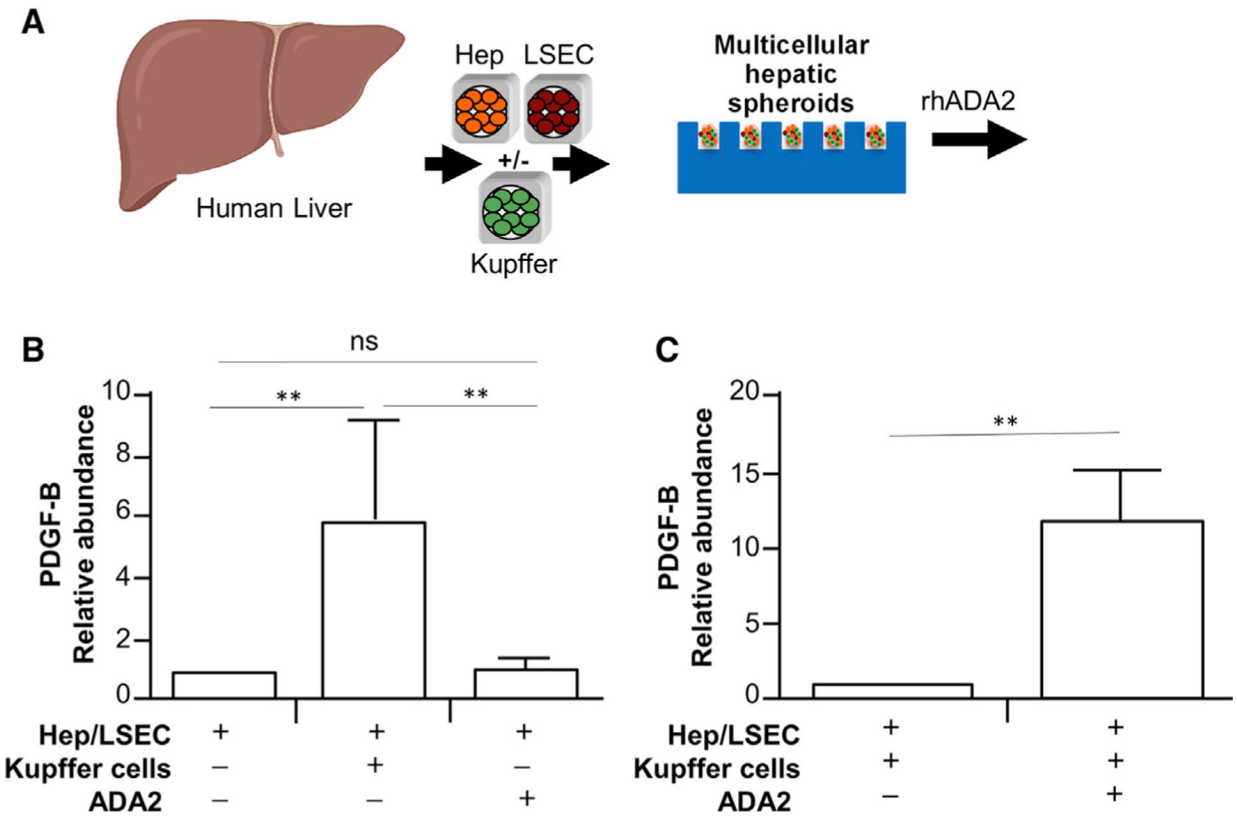

Figure 5. ADA2 enhances PDGF-B production in human hepatic Kupffer cells

(A) A diagram of the primary liver spheroid system and experiment setup.

(B) The transcription of PDGF-B in hepatocytes and Kupffer cells.

(C) The transcription of PDGF-B from Kupffer cells in response to ADA2. Error bars represent standard deviation. **p < 0.01

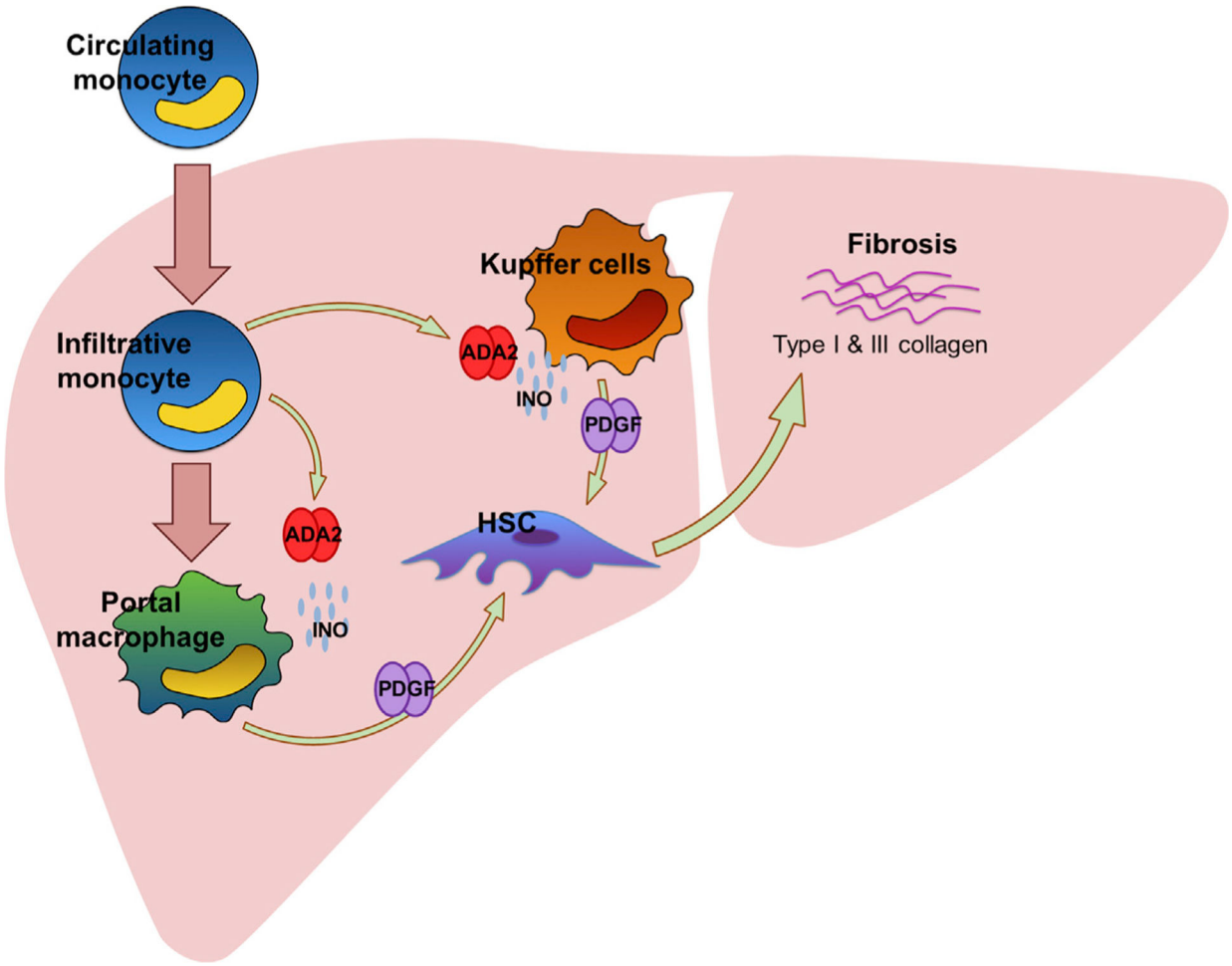

Figure 6. A model of ADA2-PDGFB axis in the infiltrative macrophages

Monocytes are recruited to the liver through chemokines. Upon their differentiation into macrophages, they release ADA2, which in turn, converts adenosine (ADO) into inosine (INO). INO further promotes the production of PDGF-BB from macrophages and Kupffer cells, which activates hepatic stellate cells (HSC) to release collagen to promote liver fibrosis.

Table 1.

Baseline characteristics of study participants

Cohort of NAFLD patients (n = 91)	
Age (mean ± sd)	56.7 ± 12.6
Gender	
Female (n, %)	37 (40.7%)
BMI (mean ± sd)	34.6 ± 6.7
NASH (n, %)	80 (87.9%)
NAS (mean, sd)	4.9 ± 1.4
Hepatic steatosis	2.0 ± 0.7
Lobular inflammation	1.4 ± 0.6
Ballooning degeneration	1.4 ± 0.7
Fibrosis (n, %)	
Stage 0	17 (18.7%)
Stage 1	22 (24.2%)
Stage 2	25 (27.5%)
Stage 3	18 (19.8%)
Stage 4	9 (9.9%)

KEY RESOURCES TABLE

Reagent or resource	Source	Identifier
Antibodies		
Anti-human CECR1	Novus	Cat# NBP1-89238, RRID:AB_11030960
Anti-human CD14	Biolegend	Cat# 301831, RRID:AB_10897803
Anti-human CD16	Abcam	ab198507 RRID: AB_2877105
Anti- human CD68	Abcam	Cat# ab955, RRID:AB_307338
Anti- human CCR2	R&D	Cat# MAB150, RRID:AB_2247178
Anti- human CCR5	R&D	Cat# MAB182, RRID:AB_2072686
Anti- human CXCR3	R&D	Cat# MAB160, RRID:AB_2086754
Anti- human PDGF-BB	Abcam	Cat# ab16829, RRID:AB_443489
Anti- human β-actin	Abcam	Cat# ab179467, RRID:AB_2737344
Anti- human Erk1/2	Cell signaling	Cat# 4695, RRID:AB_390779
Anti- human MARCO	Santa Cruz	sc-398053 RRID: AB_2893337
IRDye 800CW Goat anti-Rabbit	LI-COR Biosciences	Cat# 926-32211, RRID:AB_621843
IRDye 680RD Donkey anti-Mouse	LI-COR Biosciences	Cat# 926-68072, RRID:AB_0953628
Anti-human CD14-APC/Cy7	Biolegend	Cat# 325620, RRID:AB_830693
Anti-human CD16-PB	Biolegend	Cat# 302032, RRID:AB_2104003
Biological samples		
Human monocytes	Human peripheral blood	Primary
Human hepatocyte	Human liver resection	Primary
Human LSEC	Human liver resection	Primary
Human Kupffer cells	Human liver resection	Primary
Chemicals, peptides, and recombinant proteins		
Inosine	Sigma Aldrich	Cat# 58-63-9
Adenosine	Sigma Aldrich	Cat# 58-61-7
EHNA	Tocris	Cat# 1261/10
Recombinant human M-CSF	Peprotech	Cat# 500-P44
Critical commercial assays		
Adenosine Deaminase Assay	Diazyme	Cat# DZ117A
RNAScope Red Manual Assay 2.5 Kit	ACDBio	Cat# 322350

Reagent or resource	Source	Identifier
Pan Monocyte Isolation Kit	Miltenyi Biotec	Cat# 130-096-537
Adenosine Assay Kit	Abcam	ab211094
Inosine Assay Kit	Abcam	ab126286
Human PDGF-BB ELISA Kit	Millipore Sigma	RAB0397
Deposited data		
Sequencing data	Gene Expression Omnibus	GSE184572
Experimental models: Cell lines		
U937	ATCC	CRL-1593.2
CHO-K1	ATCC	CRL-12023
Oligonucleotides		
PDGF-B primer TTCTGAGCTCCACCTCTGGTAGGGGGAAAGTGCAGTAGGT	IDT	N/A
Beta actin primer TCCCTGGAGAAGAGCTACGAAGCACTGTGTTGGCGTACAG	IDT	N/A
TNFα primer CTCTTCTGCCTGCTGCACTTTGATGGGCTACAGGCTTGTCACTC	IDT	N/A
IL10 primer TCCTTGCTGGAGGAGGACTTTAAGGGTTGTCTGGGTCTTGGTTCTCAGCTT	IDT	N/A
IL6 primer AAATTCGGTACATCCTCGACGGCAAGTGCCTCTTTGCTGCTTTCACAC	IDT	N/A
TGFb primer ACAATTCCTGGCGATACCTCAGCACGCTAAGGCGAAAGCCCTCAATTT	IDT	N/A
ADA2 primer TGGCGTTAAGCTGCCTTACTGCTACAGGGTGGTTCCTCAA	IDT	N/A
IL1 primer CCACAGACCTTCCAGGAGAATGGTGCAGTTCAGTGATCGTACAGG	IDT	N/A
CD163 primer GCGGCTTGCAGTTTCCTCAGGCCTCCTTTTCCATTCCAGAAA	IDT	N/A
Hs-CECR1	ACDBio	Cat No. 456391
Recombinant DNA		
pDirect-Cecr1	This paper	N/A
Software and algorithms		
Stata	Stata	v.14
Prism	Graphpad	v. 5
ClusterProfiler package	R	v.3.6.0
GSEA-P	Broad Institute	MSigDB database v7.1
Image Studio Lite	LI-COR Biosciences	v.5.2.5
Cytexpert analysis software	Beckman Coulter	v.2